Majorana Doublets, Flat Bands, and Dirac Nodes in *s*-Wave Superfluids

Haiping Hu, Fan Zhang, and Chuanwei Zhang*
Department of Physics, The University of Texas at Dallas, Richardson, Texas 75080, USA

(Received 27 October 2017; revised manuscript received 14 August 2018; published 2 November 2018)

Topological superfluids protected by mirror and time-reversal symmetries are exotic states of matter possessing Majorana Kramers pairs (MKPs), yet their realizations have long been hindered by the requirement of unconventional pairing. We propose to realize such a topological superfluid by utilizing *s*-wave pairing and emergent mirror and time-reversal symmetries in two coupled 1D ultracold atomic Fermi gases with spin-orbit coupling. By stacking such systems into 2D, we discover topological and Dirac-nodal superfluids hosting distinct MKP flat bands. We show that the emergent symmetries make the MKPs and their flat bands stable against pairing fluctuations that otherwise annihilate Majorana pairs. Exploiting new experimental developments, our scheme provides a unique platform for exploring MKPs and their applications in quantum computation.

DOI: 10.1103/PhysRevLett.121.185302

Introduction.—Spin-orbit coupling (SOC) plays a crucial role in many topological quantum phenomena of condensed matter physics [1,2]. In ultracold atomic gases, SOC has been experimentally realized by coupling different hyperfine ground states through counterpropagating Raman lasers [3–13]. Due to their high controllability and zero disorder, the spin-orbit coupled ultracold atomic gases have opened a broad avenue for exploring novel topological quantum matter. In particular, the cooperation of three key ingredients, i.e., SOC, Zeeman coupling, and *s*-wave pairing interaction, can produce effective *p*-wave superfluids [14–16] that host Majorana excitations [17–19]. Because of their non-Abelian braiding statistics and potential applications in fault-tolerant quantum computing [20], topological defects containing unpaired Majorana modes have been extensively studied in solid-state systems nowadays [21–37].

These superfluids with unpaired Majorana modes belong to class D in the tenfold way of Altland-Zirnbauer classification [38,39]. Without additional symmetries, the coupling between two Majorana modes can lift their zero-energy degeneracy. Time-reversal (TR) symmetry ($\mathcal{T}^2=-1$) can, however, dictate them to form a Kramers doublet, dubbed Majorana Kramers pair (MKP) [40–43]. Topological superfluids hosting protected MKPs belong to a completely distinct symmetry class, i.e., the DIII or mirror class [42]. Intriguingly, MKPs enjoy symmetry-protected non-Abelian braiding statistics [44,45], which may constitute advantages for quantum computing.

There have been several tantalizing proposals for realizing topological superconductors hosting MKPs in solid-state materials [40–58], such as those proximitized devices exploiting the unconventional $s_{\pm}$-wave [41,58], $d_{x^2-y^2}$-wave [43], or spatially sign-switching pairing [21]. However, these schemes are challenging, as they strongly rely on the presence of exotic pairing and its fine control in materials [59]. In this context, ultracold atomic gases may provide a more controllable platform for exploring topological superfluids hosting MKPs [42]. In contrast to extrinsic proximity-induced superconductivity in solid-state platforms, superfluid orders in ultracold atomic gases are formed through intrinsic *s*-wave attractive interactions. In particular, a superfluid phase may be destroyed by quantum fluctuations in a 1D chain; therefore it is crucial to exploit weakly coupled 1D chains or 2D or 3D arrays to suppress quantum fluctuations. Yet, it has been shown that couplings between identical class D (and even class BDI [37]) chains induce edge pairing fluctuations that destroy Majorana modes [60,61]. Thus, two questions naturally arise. Can TR-invariant topological mirror superfluids be realized in ultracold atomic gases with conventional *s*-wave pairing? If so, can TR and mirror symmetries protect MKPs from pairing fluctuations? In this Letter, we address these two important questions by showing that the remarkable physics of TR-invariant topological mirror superfluids and associated MKPs can be realized in ultracold atomic gases by utilizing experimentally accessible *s*-wave pairing and synthetic 1D SOC [3–10]. Here are our main findings.

First, although the Zeeman field from Raman coupling in synthetic SOC breaks TR symmetry in a Fermi gas, effective TR and mirror symmetries emerge for two coupled gases with opposite Zeeman fields (Fig. 1), which can be realized by changing the beam profile of one Raman laser from Gaussian to Hermite-Gaussian [62]. The emergent TR and mirror symmetries, together with *s*-wave pairing, can be exploited to realize TR-invariant topological mirror superfluids [42].

Second, by tuning the Zeeman field strength and chemical potential, our 1D system undergoes various phase transitions between different phases and the topological

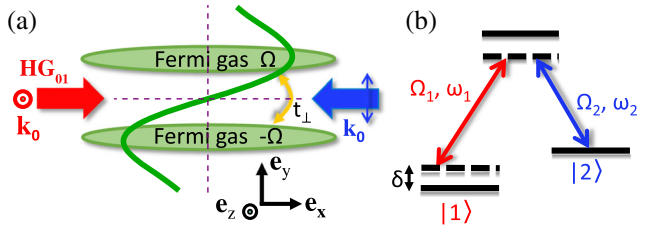

FIG. 1. Schematics of proposed experimental setups. (a) 1D SOC generated by two counterpropagating Raman lasers along $\boldsymbol{e}_x$, i.e., one HG_{01} beam (red arrow) polarized along $\boldsymbol{e}_z$ with frequency ω_1 and one Gaussian beam (blue arrow) polarized along $\boldsymbol{e}_y$ with frequency ω_2. The green line shows the resulting Zeeman field along $\boldsymbol{e}_y$. (b) Two-photon process induced by the two Raman lasers in (a) with a detuning δ.

superfluid characterized by a $\mathbb{Z}_2$ invariant and the emergence of MKPs. Even though the SOC is 1D, our 2D system exhibits both topological and Dirac-nodal [63] superfluids hosting distinct flat bands of MKPs. This extension strongly suppresses quantum fluctuations that may destroy the two superfluid phases.

Third, as evidenced by our self-consistent calculations [64–69], the degeneracies of MKPs and their flat bands are symmetry protected against pairing fluctuations, which are known to annihilate Majorana pairs for coupled 1D chains. (All of these results also apply to the 3D case.) Therefore, our scheme provides a simple experimentally feasible route for realizing TR-invariant topological and Dirac-nodal superfluids, paving the way for observing MKPs and exploring their non-Abelian statistics [44,45] and interaction effects [46,47].

Model.—Consider two coupled 1D Fermi gases of ultracold atoms with the same SOC but opposite Zeeman fields. (A double-well trapping potential along $\hat{y}$ is used to create this system.) As sketched in Fig. 1, the SOC can be achieved by two counterpropagating Raman lasers coupling two atomic hyperfine states $|1\rangle$ and $|2\rangle$. This setup is the same as those in previous experiments [3–13], except that one laser beam is changed from Gaussian to Hermite-Gaussian HG_{01} mode [62], and can be described by the Hamiltonian $h_k = \hbar^2 k^2/2m + \Omega\sigma_z + \delta\sigma_y + 2\alpha k\sigma_y$ in a rotated basis with $|1,2\rangle = (|\uparrow\rangle \pm i|\downarrow\rangle)/\sqrt{2}$. Here k is the quasimomentum in each gas, α is the SOC strength, δ is the two-photon detuning, and $\Omega = \Omega_0 y \exp(-y^2/w^2)$ is the position-dependent Raman coupling serving as the Zeeman field. Given the antisymmetric HG_{01} beam, the Zeeman field is opposite at the two gases, which is crucial for realizing an emergent TR symmetry.

Taking into account the s-wave interaction induced superfluidity, the physics of our 1D Fermi gas system can be described by the Bogoliubov–de Gennes (BdG) Hamiltonian [70] $H_k = \Psi_k^\dagger \mathcal{H}_k^{BdG} \Psi_k/2$ with

$$\mathcal{H}_k^{\mathrm{BdG}} = [\xi_k + 2\alpha \sin k\sigma_y - t_\perp s_x]\tau_z + \Omega\sigma_z s_z + \Delta\tau_x \quad (1)$$

expressed in the Nambu spinor basis $\Psi_k = (\phi_k, i\sigma_y\phi_{-k}^\dagger)$. Here $\phi_k = (c_{k\uparrow,1}, c_{k\downarrow,1}, c_{k\uparrow,2}, c_{k\downarrow,2})^T$ with $c_{k\sigma,s}$ the fermion annihilation operators; $\boldsymbol{\sigma}$, $\boldsymbol{s}$, and $\boldsymbol{\tau}$ are Pauli matrices acting on the fermion spin, double chain, and particle-hole spaces, respectively; $\xi_k = -2t\cos k - \mu$ is the intrachain kinetic energy with a chemical potential μ, $t_\perp$ is the inter-chain coupling, and $\delta = 0$ has been chosen for the detuning. The lattice regularization of the free-space fermion kinetic energy would not change any essential physics [70]. Importantly, the Zeeman field $\Omega\sigma_z s_z$ is exactly opposite for the two chains, and the s-wave pairing order parameter Δ must be self-consistently determined [64–69]. Diagonalizing the Hamiltonian [Eq. (1)], we obtain the quasiparticle energy spectrum

$$E(k) = \pm[(2\alpha \sin k \pm t_\perp)^2 + \Omega^2 + \Delta^2 + \xi_k^2 \pm 2\sqrt{(\Delta^2 + \xi_k^2)\Omega^2 + (2\alpha \sin k \pm t_\perp)^2 \xi_k^2}]^{1/2}, \quad (2)$$

with twofold degeneracies at $k = 0$ and π due to an emergent TR symmetry, as we elaborate below.

Symmetry and invariant.—The model [Eq. (1)] has three independent symmetries that govern the underlying physics. First, there is an intrinsic particle-hole symmetry reflecting the BdG redundancy: $\mathcal{P}\mathcal{H}_k^{\mathrm{BdG}}\mathcal{P}^{-1} = -\mathcal{H}_{-k}^{\mathrm{BdG}}$ with $\mathcal{P} = \tau_y\sigma_y\mathcal{K}$ and $\mathcal{K}$ the complex conjugation. Second, even though the TR symmetry is explicitly broken by the Zeeman field within each chain, Eq. (1) is still invariant under TR followed by chain inversion, i.e.,

$$\tilde{\mathcal{T}}\mathcal{H}_k^{\mathrm{BdG}}\tilde{\mathcal{T}}^{-1} = \mathcal{H}_{-k}^{\mathrm{BdG}}, \qquad \tilde{\mathcal{T}} = is_x\sigma_y\mathcal{K}. \quad (3)$$

Given that $\tilde{\mathcal{T}}^2 = -1$, such an emergent TR symmetry dictates the Kramers degeneracies found in the spectrum [Eq. (2)] at $k = 0$ and π. Note that the composite operation of $\mathcal{P}$ and $\tilde{\mathcal{T}}$ also leads to a chiral symmetry: $\mathcal{C}\mathcal{H}_k^{\mathrm{BdG}}\mathcal{C}^{-1} = -\mathcal{H}_k^{\mathrm{BdG}}$ with $\mathcal{C} = \mathcal{P}\tilde{\mathcal{T}}$. Third, the setup has a mirror symmetry such that the two chains are the mirror images of each other, i.e.,

$$\mathcal{M}\mathcal{H}_k^{\mathrm{BdG}}\mathcal{M}^{-1} = \mathcal{H}_k^{\mathrm{BdG}}, \qquad \mathcal{M} = is_x\sigma_y. \quad (4)$$

Since the mirror symmetry with $\mathcal{M}^2 = -1$ is a spatial symmetry, naturally $[\mathcal{M}, \mathcal{O}] = 0$ with $\mathcal{O} = \mathcal{P}$, $\tilde{\mathcal{T}}$ and $\mathcal{C}$.

In light of the above symmetry analysis, the Hamiltonian [Eq. (1)] belongs to both the DIII class [38,39] and the mirror class [42] in topological classification. It follows that a $\mathbb{Z}_2$ index ν [70,71] and a mirror winding number γ_m, with $\nu = \gamma_m \bmod 2$ [42], can both be used for characterizing the band topology of model [Eq. (1)].

We find that the transitions between topologically distinct phases occur at the phase boundary where

$$\xi_k^2 + \Delta^2 = \Omega^2, \qquad 4\alpha^2 \sin^2 k = t_\perp^2. \quad (5)$$

For $t_\perp = 0$, the quasiparticle gap closes at $k = 0$, and the phase boundary reduces to that of single-chain superfluids [22,23]. For a finite $t_\perp$, the quasiparticle gap closes at a finite k, and the critical Zeeman fields read

$$\Omega_{\pm} = [(2t\sqrt{1 - t_{\perp}^2/4\alpha^2} \pm \mu)^2 + \Delta^2]^{1/2}. \quad (6)$$

Applying the established formulas for ν [70,71] and γ_m [42] to Eq. (1), we conclude that

$$\nu = \gamma_m = \begin{cases} 1 & \text{if } \Omega_- < |\Omega| < \Omega_+, \\ 0 & \text{otherwise.} \end{cases} \quad (7)$$

Our model in the nontrivial regime realizes not only a TR-invariant topological superfluid but also the first topological mirror superfluid [42] in degenerate gases.

Self-consistent phase diagram.—In ultracold atomic gases, the local s-wave pair potential in real space must be determined in a self-consistent manner [64–69], together with the quasiparticle energies and wave functions. In our numerical calculations [70], the chemical potential is fixed without loss of generality, and the open boundary condition is used for the purpose of observing MKPs. We choose $L = 120$ as the length of chain, t as the energy unit, and $\langle\Delta\rangle = \sum_i |\Delta_i|/L$ as the pairing strength.

Figure 2(a) plots the phase diagram in the Ω-μ plane, which is symmetric with respect to $\mu = 0$ and $\Omega = 0$. Evidently, the numerical phase boundaries are in good harmony with those determined by Eq. (5). In total, there are five distinct phases: the normal superfluid, topological superfluid, metal with SOC, polarized insulator, and trivial vacuum. The vacuum state occurs when $|\mu|$ is too large to cross the single-particle bands. The system becomes the polarized insulator near $|\mu| = 0$ if the Zeeman field strength $|\Omega|$ is sufficiently large; each lattice site per chain is occupied by one fermion of the same polarization. At relatively smaller $|\Omega|$ and $|\mu|$, superfluidity spontaneously emerges with a finite bulk pairing gap for quasiparticle excitations. In this regime, whereas it is the normal superfluid without any boundary zero mode if both $|\Omega|$ and $|\mu|$ approach zero, it becomes the topological superfluid with two degenerate zero modes per boundary, i.e., the MKP, if $|\mu|$ approaches to the original band degeneracies and if $|\Omega| > \Omega_-$ as required in Eq. (7). As $|\Omega|$ further increases, the superfluidity gradually vanishes, and the metal phase emerges with an excitation gap scales linearly with $1/L$.

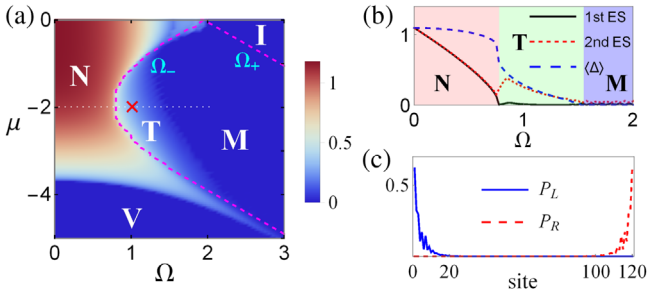

FIG. 2. (a) Phase diagram in the Ω-μ plane, symmetric with respect to $\mu = 0$ and $\Omega = 0$. The contour plot shows the site-averaged pairing $\langle\Delta\rangle$ in the normal superfluid (N), topological superfluid (T), metal with SOC (M), polarized insulator (I), and trivial vacuum (V). The dotted red lines are the phase boundaries determined by Eq. (5). (b) Phase transitions along the white dotted line in (a). The black solid (red dotted) lines denote the first (second) quasiparticle excitation states (ES) in the spectrum, both of which are twofold degenerate. (c) Probability distributions of the left (L) and right (R) MKPs at the red cross in (a). $\sum_i P_L(i) = \sum_i P_R(i) = 2$ are the hallmarks of MKPs. $\alpha = 1$ and $t_\perp = 0.5$ are used in (a)–(c).

Figure 2(b) with $\mu = -2$ features the most appealing part of the phase diagram, where there are two successive phase transitions as Ω increases from 0. The first transition occurs at $\Omega = \Omega_-$: the normal superfluid turns to the topological superfluid with the emergence of one localized MKP per boundary, as shown in Fig. 2(c). As Ω becomes stronger, the pairing strength $\langle\Delta\rangle$ becomes weaker. Eventually at the second transition, $\langle\Delta\rangle$ vanishes and the system enters into the metal phase with gapless single-particle excitations.

2D topological superfluids.—By stacking our double chains, we can obtain exotic 2D and 3D topological superfluids protected by the emergent TR and mirror symmetries. The extension to higher dimensions can suppress quantum fluctuations and stabilize long-range pairing orders. We focus on the 2D case [70], and the 3D generalization is straightforward. The staggered Zeeman field switches sign between neighboring chains along $\hat{y}$. This setup can be described by the BdG Hamiltonian

$$\mathcal{H}_{\boldsymbol{k}}^{\mathrm{BdG}} = [\xi_{k_x} + 2\alpha \sin k_x \sigma_y - (t_1 + t_2 \cos k_y) s_x - t_2 \sin k_y s_y]\tau_z + \Omega s_z \sigma_z + \Delta \tau_x, \quad (8)$$

where t_1 and t_2 are the alternating interchain couplings along $\hat{y}$. Such a system has an emergent property

$$\tilde{\mathcal{T}} \mathcal{H}^{\mathrm{BdG}}(k_x, k_y) \tilde{\mathcal{T}}^{-1} = \mathcal{H}^{\mathrm{BdG}}(-k_x, k_y); \quad (9)$$

i.e., the system respects the TR symmetry in Eq. (3) and belongs to class DIII with a $\mathbb{Z}_2$ invariant ν_{k_y} for any k_y, which is an anomalous pumping parameter [44].

Consequently, there can be three distinct phases for Eq. (8). Whereas the superfluid is normal if $\nu_{k_y} = 0$ for any k_y, an unprecedented topological superfluid emerges if $\nu_{k_y} = 1$ for any k_y. Remarkably in the topological phase, there emerges a flat band of MKPs at the edge along $\hat{y}$, because there is a MKP corresponding to the nontrivial $\mathbb{Z}_2$ invariant for any k_y. (This edge flat band is a consequence of the bulk topological property, and the band flatness is protected by the TR and mirror symmetries, although the edge flat band itself may be trivial [72] if treated as a 1D system.) Intriguingly, if $\nu_0 \neq \nu_\pi$, a nodal superfluid emerges. As the $\mathbb{Z}_2$ invariant changes from $k_y = 0$ to $k_y = \pi$, the bulk gap must close at least one k_y in between 0 and π, separating the $\nu = 0$ and $\nu = 1$ regimes, and a flat band of MKPs emerge between the projected nodes [63] at the edge along $\hat{y}$.

Figure 3(a) illustrates a representative phase diagram in the Ω-Δ plane. Indeed, all three phases emerge and the

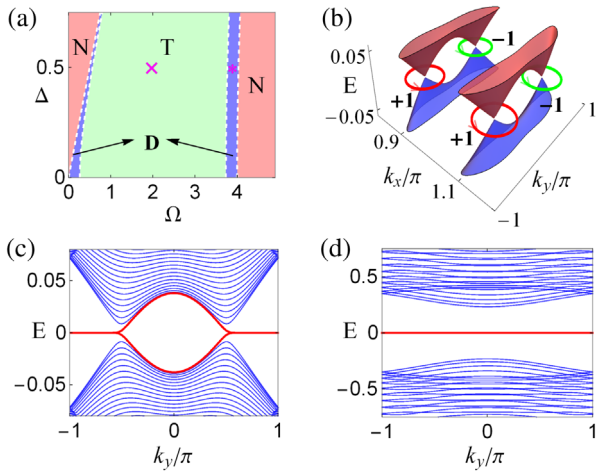

FIG. 3. (a) Phase diagram in the Ω-Δ plane for the 2D model [Eq. (8)]. The red, green, and blue regions denote the normal (N), topological (T), and Dirac-nodal (D) superfluids, respectively. (b) Bulk quasiparticle spectrum for the Dirac superfluid labeled by the red star in (a). Each Dirac point is indexed by a winding number $\gamma_t = \pm 1$. (c) and (d) Quasiparticle spectrum with MKP edge flat bands under open boundary condition for the Dirac and topological superfluids labeled in (a). $t_1 = t_2 = 0.5$, $\alpha = 1$, and $\mu = -2$ are used in (a)–(d).

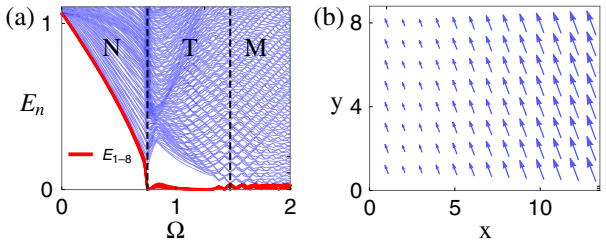

FIG. 4. (a) Self-consistent quasiparticle spectrum for the 100×8 lattice model. The red lines denote the eight lowest quasiparticle excitation states. (b) Vector plot of the local pairing fields $\Delta_j e^{i\phi_j}$ for $\Omega = 1.1$. The length (direction) of each arrow denotes the strength (phase) of the local pairing field. $t_1 = t_2 = 0.5$, $\alpha = 1$, and $\mu = -2$ are used in (a) and (b).

nodal superfluid intervenes the normal and topological ones. Surprisingly, we find that the nodes are Dirac points with linear dispersions and topological protections. Diagonalizing Eq. (8) yields the phase boundaries and the Dirac point positions, as determined by

$$\xi_{k_x}^2 + \Delta^2 = \Omega^2, \quad 4\alpha^2 \sin^2 k_x = t_1^2 + t_2^2 + 2t_1 t_2 \cos k_y. \quad (10)$$

The Dirac points are twofold degenerate and come in multiples of four, as dictated by the $\tilde{\mathcal{T}}$ and $\mathcal{M}$ symmetries that respectively flip k_x and k_y. Moreover, any loop enclosing one such Dirac point has a total winding number $\gamma_t = \pm 1$ [63], protected by an emergent chiral symmetry

$$\tilde{\mathcal{C}} \mathcal{H}_{\boldsymbol{k}}^{\mathrm{BdG}} \tilde{\mathcal{C}}^{-1} = -\mathcal{H}_{\boldsymbol{k}}^{\mathrm{BdG}}, \qquad \tilde{\mathcal{C}} = \tau_y \sigma_y. \quad (11)$$

Figure 3(b) displays the four Dirac points and their γ_ts accordingly. Figures 3(c) and 3(d) contrast the MKP edge flat bands in the Dirac-nodal and topological superfluids.

Discussion.—It is instructive to consider the stability of MKPs and their flat bands in our proposed scheme. For an array of topological superfluids without the $\tilde{\mathcal{T}}$ and $\mathcal{M}$ symmetries, it is known that Majorana interactions spontaneously produce nonuniform pairing fields $\Delta_j e^{i\phi_j}$ and edge supercurrent loops [61]. Since the phase fluctuations cannot be gauged away, the Majorana modes can be gapped out in pairs. Neglecting long-range interactions, the Majorana annihilation is governed by the nearest-neighbor Josephson couplings as follows [60]:

$$\delta H = -\sum_{\langle ij \rangle} [J_0 \cos \phi_{ij} + i J_{ij} \gamma_i \gamma_j \sin(\phi_{ij}/2)], \quad (12)$$

with J_0, $J_{ij} > 0$ and $\phi_{ij} = \phi_i - \phi_j$. While the first term favors a global phase coherence, the second term splits the Majorana zero modes through phase fluctuations.

In sharp contrast, the MKP flat bands of our system are robust against such phase fluctuations. This can be best understood from the symmetry perspective. Under the $\mathcal{M}$ operation, the local pairing term $\Delta_i e^{i\phi_i} c_{i\uparrow} c_{i\downarrow}$ becomes $\Delta_i e^{i\phi_i} c_{i+1\uparrow} c_{i+1\downarrow}$ since the sublattice and spin indices in Eq. (8) are simultaneously flipped. For the Josephson coupling, the J_{ij} term must vanish as $\phi_i = \phi_{i+1}$ is dictated by mirror symmetry.

Our self-consistent calculations also agree with such a symmetry argument. Figure 4(a) plots the BdG spectrum for a 100×8 lattice model of Eq. (8). Consistent with Fig. 3(a), the system undergoes two transitions as the Zeeman field increases: from a normal superfluid to a topological one and eventually to a metal phase with $\langle \Delta \rangle = 0$. (Dirac points are absent due to the finite size effect.) The topological phase hosts eightfold degenerate zero modes on the boundary along $\hat{y}$, forming a MKP flat band that is also stable against the t_1-t_2 anisotropy. These remarkable features suggest that our proposed scheme is superior to previous ones.

Finally, a few comments are in order on relevant experiments. In the 2D setup, the Zeeman field switches signs between neighboring chains of distance b. This can be realized through the periodic modulation $\Omega_1 \sim \cos(\pi y/b)$ for one Raman laser. Such a modulation can be produced by a digital micromirror device [70,73,74], which can generate an arbitrary modulation of laser intensity. This setup can be generalized to a 3D lattice with $\Omega_1 \sim \cos(\pi y/b) \cos(\pi z/c)$, where a boundary MKP flat band is anticipated. Our scheme of restoring TR symmetry via a spatial reflection can be generalized to various different systems, where the SOCs have been realized for other types of pseudospin states [75–78].

The MKPs can be experimentally detected using spatially resolved radio-frequency spectroscopy [70,79–83], which measures the local density of states, similar to scanning tunneling microscope. Different from a single

Majorana mode, the intrinsic twofold degeneracy of a MKP can be further affirmed from the energy splitting and spatial separation of two Majorana modes due to symmetry breaking [70], which can be induced by the imbalance of Ω between the two chains. Our results not only provide a simple experimental scheme for realizing mirror- and TR-invariant topological and Dirac-nodal superfluids, but also establish a unique platform for exploring MKPs and their applications in quantum computation.

H. H. and C. Z. are supported by NSF (PHY-1505496, PHY-1806227), ARO (W911NF-17-1-0128), and AFOSR (FA9550-16-1-0387). F. Z. is supported by UTD (Research Enhancement Funds) and ARO (W911NF-18-1-0416).

Note added.—Near the submission of this manuscript, we became aware of an independent work [84] that explores MKPs in double semiconductor nanowires with proximity-induced *s*-wave pairing and *ad hoc* opposite Zeeman fields. While pairing fluctuation, mirror symmetry, Dirac phase, and flat band are not discussed in Ref. [84], the results based on the emergent time-reversal symmetry in the two works agree with each other.

*chuanwei.zhang@utdallas.edu

[1] M. Z. Hasan and C. L. Kane, Colloquium: Topological insulators, Rev. Mod. Phys. **82**, 3045 (2010).
[2] X.-L. Qi and S.-C. Zhang, Topological insulators and superconductors, Rev. Mod. Phys. **83**, 1057 (2011).
[3] Y.-J. Lin, K. Jiménez-García, and I. B. Spielman, Spin-orbit-coupled Bose-Einstein condensates, Nature (London) **471**, 83 (2011).
[4] Z. K. Fu, P. J. Wang, S. J. Chai, L. H. Huang, and J. Zhang, Bose-Einstein condensate in a light-induced vector gauge potential using 1064-nm optical-dipole-trap lasers, Phys. Rev. A **84**, 043609 (2011).
[5] J.-Y. Zhang *et al.*, Collective Dipole Oscillations of a Spin-Orbit Coupled Bose-Einstein Condensate, Phys. Rev. Lett. **109**, 115301 (2012).
[6] C. Qu, C. Hamner, M. Gong, C. Zhang, and P. Engels, Observation of Zitterbewegung in a spin-orbit coupled Bose-Einstein condensate, Phys. Rev. A **88**, 021604(R) (2013).
[7] A. J. Olson, S.-J. Wang, R. J. Niffenegger, C.-H. Li, C. H. Greene, and Y. P. Chen, Tunable Laudan-Zener transitions in a spin-orbit-coupled Bose-Einstein condensate, Phys. Rev. A **90**, 013616 (2014).
[8] P. Wang, Z.-Q. Yu, Z. Fu, J. Miao, L. Huang, S. Chai, H. Zhai, and J. Zhang, Spin-Orbit Coupled Degenerate Fermi Gases, Phys. Rev. Lett. **109**, 095301 (2012).
[9] L. W. Cheuk, A. T. Sommer, Z. Hadzibabic, T. Yefsah, W. S. Bakr, and M. W. Zwierlein, Spin-Injection Spectroscopy of a Spin-Orbit Coupled Fermi Gas, Phys. Rev. Lett. **109**, 095302 (2012).
[10] R. A. Williams, M. C. Beeler, L. J. LeBlanc, and I. B. Spielman, Raman-Induced Interactions in a Single-Component Fermi Gas Near an *s*-Wave Feshbach Resonance, Phys. Rev. Lett. **111**, 095301 (2013).
[11] L. Huang, Z. Meng, P. Wang, P. Peng, S.-L. Zhang, L. Chen, D. Li, Q. Zhou, and J. Zhang, Experimental realization of two-dimensional synthetic spin-orbit coupling in ultracold Fermi gases, Nat. Phys. **12**, 540 (2016).
[12] Z. Meng, L. Huang, P. Peng, D. Li, L. Chen, Y. Xu, C. Zhang, P. Wang, and J. Zhang, Experimental Observation of a Topological Band Gap Opening in Ultracold Fermi Gases with Two-Dimensional Spin-Orbit Coupling, Phys. Rev. Lett. **117**, 235304 (2016).
[13] Z. Wu, L. Zhang, W. Sun, X.-T. Xu, B.-Z. Wang, S.-C. Ji, Y. Deng, S. Chen, X.-J. Liu, and J.-W. Pan, Realization of two-dimensional spin-orbit coupling for Bose-Einstein condensates, Science **354**, 83 (2016).
[14] C. Zhang, S. Tewari, R. M. Lutchyn, and S. D. Sarma, $p_x + ip_y$ Superfluid from *s*-Wave Interactions of Fermionic Cold Atoms, Phys. Rev. Lett. **101**, 160401 (2008).
[15] M Sato, Y. Takahashi, and S. Fujimoto, Non-Abelian Topological Order in *s*-Wave Superfluids of Ultracold Fermionic Atoms, Phys. Rev. Lett. **103**, 020401 (2009).
[16] L. Jiang, T. Kitagawa, J. Alicea, A. R. Akhmerov, D. Pekker, G. Refael, J. I. Cirac, E. Demler, M. D. Lukin, and P. Zoller, Majorana Fermions in Equilibrium and in Driven Cold-Atom Quantum Chains, Phys. Rev. Lett. **106**, 220402 (2011).
[17] F. Wilczek, Majorana returns, Nat. Phys. **5**, 614 (2009).
[18] J. Alicea, New directions in the pursuit of Majorana fermions in solid state systems, Rep. Prog. Phys. **75**, 076501 (2012).
[19] M. Franz, Majorana's wires, Nat. Nanotechnol. **8**, 149 (2013).
[20] A. Y. Kitaev, Fault-tolerant quantum computation by anyons, Ann. Phys. (Amsterdam) **303**, 2 (2003).
[21] L. Fu and C. L. Kane, Superconducting Proximity Effect and Majorana Fermions at the Surface of a Topological Insulator, Phys. Rev. Lett. **100**, 096407 (2008).
[22] R. M. Lutchyn, J. D. Sau, and S. D. Sarma, Majorana Fermions and a Topological Phase Transition in Semiconductor-Superconductor Heterostructures, Phys. Rev. Lett. **105**, 077001 (2010).
[23] Y. Oreg, G. Refael, and F. von Oppen, Helical Liquids and Majorana Bound States in Quantum Chains, Phys. Rev. Lett. **105**, 177002 (2010).
[24] J. D. Sau, R. M. Lutchyn, S. Tewari, and S. D. Sarma, Generic New Platform for Topological Quantum Computation Using Semiconductor Heterostructures, Phys. Rev. Lett. **104**, 040502 (2010).
[25] S. Tewari, S. D. Sarma, C. Nayak, C. Zhang, and P. Zoller, Quantum Computation Using Vortices and Majorana Zero Modes of a $p_x + ip_y$ Superfluid of Fermionic Cold Atoms, Phys. Rev. Lett. **98**, 010506 (2007).
[26] J. Alicea, Majorana fermions in a tunable semiconductor device, Phys. Rev. B **81**, 125318 (2010).
[27] T. D. Stanescu, R. M. Lutchyn, and S. D. Sarma, Majorana fermions in semiconductor nanochains, Phys. Rev. B **84**, 144522 (2011).
[28] J. Alicea, Y. Oreg, G. Refael, F. von Oppen, and M. P. A. Fisher, Non-Abelian statistics and topological quantum information processing in 1D chain networks, Nat. Phys. **7**, 412 (2011).

[29] X.-L. Qi, T. L. Hughes, and S.-C. Zhang, Chiral topological superconductor from the quantum Hall state, Phys. Rev. B **82**, 184516 (2010).
[30] A. C. Potter and P. A. Lee, Multichannel Generalization of Kitaev's Majorana End States and a Practical Route to Realize them in Thin Films, Phys. Rev. Lett. **105**, 227003 (2010).
[31] V. Mourik, K. Zuo, S. M. Frolov, S. R. Plissard, E. P. A. M. Bakkers, and L. P. Kouwenhoven, Signatures of Majorana fermions in hybrid superconductor-semiconductor nanochain devices, Science **336**, 1003 (2012).
[32] S. Nadj-Perge, I. K. Drozdov, J. Li, H. Chen, S. Jeon, J. Seo, A. H. MacDonald, B. A. Bernevig, and A. Yazdani, Observation of Majorana fermions in ferromagnetic atomic chains on a superconductor, Science **346**, 602 (2014).
[33] A. Das, Y. Ronen, Y. Most, Y. Oreg, M. Heiblum, and H. Shtrikman, Zero-bias peaks and splitting in an Al-InAs nanochain topological superconductor as a signature of Majorana fermions, Nat. Phys. **8**, 887 (2012).
[34] H. O. H. Churchill, V. Fatemi, K. Grove-Rasmussen, M. T. Deng, P. Caroff, H. Q. Xu, and C. M. Marcus, Superconductor-nanochain devices from tunneling to the multichannel regime: Zero-bias oscillations and magnetoconductance crossover, Phys. Rev. B **87**, 241401(R) (2013).
[35] M.-X. Wang *et al.*, The coexistence of superconductivity and topological order in the Bi_2Se_3 thin films, Science **336**, 52 (2012).
[36] A. D. K. Finck, D. J. Van Harlingen, P. K. Mohseni, K. Jung, and X. Li, Anomalous Modulation of a Zero-Bias Peak in a Hybrid Nanochain-Superconductor Device, Phys. Rev. Lett. **110**, 126406 (2013).
[37] S. Tewari and J. D. Sau, Topological Invariants for Spin-Orbit Coupled Superconductor Nanowires, Phys. Rev. Lett. **109**, 150408 (2012).
[38] A. P. Schnyder, S. Ryu, A. Furusaki, and A. W. W. Ludwig, Classification of topological insulators and superconductors, AIP Conf. Proc. **1134**, 10 (2009).
[39] A. Kitaev, Periodic table for topological insulators and superconductors, AIP Conf. Proc. **1134**, 22 (2009).
[40] X.-L. Qi, T. L. Hughes, S. Raghu, and S.-C. Zhang, Time-Reversal-Invariant Topological Superconductors and Superfluids in Two and Three Dimensions, Phys. Rev. Lett. **102**, 187001 (2009).
[41] F. Zhang, C. L. Kane, and E. J. Mele, Time-Reversal-Invariant Topological Superconductivity and Majorana Kramers Pairs, Phys. Rev. Lett. **111**, 056402 (2013).
[42] F. Zhang, C. L. Kane, and E. J. Mele, Topological Mirror Superconductivity, Phys. Rev. Lett. **111**, 056403 (2013).
[43] C. L. M. Wong and K. T. Law, Majorana Kramers doublets in $d_{x^2-y^2}$-wave superconductors with Rashba spin-orbit coupling, Phys. Rev. B **86**, 184516 (2012).
[44] F. Zhang and C. L. Kane, Anomalous topological pumps and fractional Josephson effects, Phys. Rev. B **90**, 020501(R) (2014).
[45] X.-J. Liu, C. L. M. Wong, and K. T. Law, Non-Abelian Majorana Doublets in Time-Reversal-Invariant Topological Superconductors, Phys. Rev. X **4**, 021018 (2014).
[46] F. Zhang and C. L. Kane, Time-Reversal-Invariant Z_4 Fractional Josephson Effect, Phys. Rev. Lett. **113**, 036401 (2014).
[47] Z.-q. Bao and F. Zhang, Topological Majorana Two-Channel Kondo Effect, Phys. Rev. Lett. **119**, 187701 (2017).
[48] C.-X. Liu and B. Trauzettel, Helical Dirac-Majorana interferometer in a superconductor/topological insulator sandwich structure, Phys. Rev. B **83**, 220510(R) (2011).
[49] S. Nakosai, Y. Tanaka, and N. Nagaosa, Topological Superconductivity in Bilayer Rashba System, Phys. Rev. Lett. **108**, 147003 (2012).
[50] S. Deng, L. Viola, and G. Ortiz, Majorana Modes in Time-Reversal Invariant *s*-Wave Topological Superconductors, Phys. Rev. Lett. **108**, 036803 (2012).
[51] S. Nakosai, J. C. Budich, Y. Tanaka, B. Trauzettel, and N. Nagaosa, Majorana Bound States and Nonlocal Spin Correlations in a Quantum Chain on an Unconventional Superconductor, Phys. Rev. Lett. **110**, 117002 (2013).
[52] A. Keselman, L. Fu, A. Stern, and E. Berg, Inducing Time-Reversal-Invariant Topological Superconductivity and Fermion Parity Pumping in Quantum Chains, Phys. Rev. Lett. **111**, 116402 (2013).
[53] E. Gaidamauskas, J. Paaske, and K. Flensberg, Majorana Bound States in Two-Channel Time-Reversal-Symmetric Nanochain Systems, Phys. Rev. Lett. **112**, 126402 (2014).
[54] J. Wang, Y. Xu, and S.-C. Zhang, Two-dimensional time-reversal-invariant topological superconductivity in a doped quantum spin-Hall insulator, Phys. Rev. B **90**, 054503 (2014).
[55] J. Klinovaja, A. Yacoby, and D. Loss, Kramers pairs of Majorana fermions and parafermions in fractional topological insulators, Phys. Rev. B **90**, 155447 (2014).
[56] C. Schrade, A. A. Zyuzin, J. Klinovaja, and D. Loss, Proximity-Induced π Josephson Junctions in Topological Insulators and Kramers Pairs of Majorana Fermions, Phys. Rev. Lett. **115**, 237001 (2015).
[57] Y. Y. Huang and C.-K. Chiu, Helical Majorana edge mode in a superconducting antiferromagnetic quantum spin Hall insulator, Phys. Rev. B **98**, 081412 (2018).
[58] Q. Wang, C.-C. Liu, Y.-M. Lu, and F. Zhang, High-Temperature Majorana Corner States, Phys. Rev. Lett. **121**, 186801 (2018).
[59] Click to see the proposed no-go theorem, online.kitp.ucsb.edu/online/spintronics13/zhang/oh/09.html.
[60] Y. Li, D. Wang, and C. Wu, Spontaneous breaking of time-reversal symmetry in the orbital channel for the boundary Majorana flat bands, New J. Phys. **15**, 085002 (2013).
[61] D. Wang, Z. S. Huang, and C. Wu, The fate and remnant of Majorana zero modes in a quantum chain array, Phys. Rev. B **89**, 174510 (2014).
[62] T. P. Meyrath, F. Schreck, J. L. Hanssen, C.-S. Chuu, and M. G. Raizen, A high frequency optical trap for atoms using Hermite-Gaussian beams, Opt. Express **13**, 2843 (2005).
[63] S. A. Yang, H. Pan, and F. Zhang, Dirac and Weyl Superconductors in Three Dimensions, Phys. Rev. Lett. **113**, 046401 (2014).
[64] J. Brand, L. A. Toikka, and U. Zuelicke, Accurate projective two-band description of topological superfluidity in spin-orbit-coupled Fermi gases, SciPost Phys. **5**, 016 (2018).
[65] C. Qu, Z. Zheng, M. Gong, Y. Xu, L. Mao, X. Zou, G. Guo, and C. Zhang, Topological superfluids with

finite-momentum pairing and Majorana fermions, Nat. Commun. **4**, 2710 (2013).
[66] Y. Xu, C. Qu, M. Gong, and C. Zhang, Competing superfluid orders in spin-orbit-coupled fermionic cold-atom ical lattices, Phys. Rev. A **89**, 013607 (2014).
[67] C. Qu, M. Gong, and C. Zhang, Fulde-Ferrell-Larkin-Ovchinnikov or Majorana superfluids: The fate of fermionic cold atoms in spin-orbit-coupled optical lattices, Phys. Rev. A **89**, 053618 (2014).
[68] Y. Xu, L. Mao, B. Wu, and C. Zhang, Dark Solitons with Majorana Fermions in Spin-Orbit-Coupled Fermi Gases, Phys. Rev. Lett. **113**, 130404 (2014).
[69] L. Jiang, E. Tiesinga, X.-J. Liu, H. Hu, and H. Pu, Spin-orbit-coupled topological Fulde-Ferrell states of fermions in a harmonic trap, Phys. Rev. A **90**, 053606 (2014).
[70] See Supplemental Materials at http://link.aps.org/supplemental/10.1103/PhysRevLett.121.185302 for more discussions on the topological invariants, validity of the double-chain model, continuum models, and experimental detections.
[71] J. C. Budich and E. Ardonne, Topological invariant for generic one-dimensional time-reversal-symmetric superconductors in class DIII, Phys. Rev. B **88**, 134523 (2013).
[72] L. Chen, T. Mazaheri, A. Seidel, and X. Tang, The impossibility of exactly flat non-trivial Chern bands in strictly local periodic tight binding models, J. Phys. A **47**, 152001 (2014).
[73] P. Zupancic, P. M. Preiss, R. Ma, A. Lukin, M. E. Tai, M. Rispoli, R. Islam, and M. Greiner, Ultra-precise holographic beam shaping for microscopic quantum control, Opt. Express **24**, 13881 (2016).
[74] M. E. Tai, A. Lukin, M. Rispoli, R. Schittko, T. Menke, D. Borgnia, P. M. Preiss, F. Grusdt, A. M. Kaufman, and M. Greiner, Microscopy of the interacting Harper–Hofstadter model in the two-body limit, Nature (London) **546**, 519 (2017).
[75] J.-R. Li, J. Lee, W. Huang, S. Burchesky, B. Shteynas, F. Ç. Top, A. O. Jamison, and W. Ketterle, A stripe phase with supersolid properties in spin-orbit-coupled Bose-Einstein condensates, Nature (London) **543**, 91 (2017).
[76] J. Li, W. Huang, B. Shteynas, S. Burchesky, F. Ć. Top, E. Su, J. Lee, A. O. Jamison, and W. Ketterle, Spin-Orbit Coupling and Spin Textures in Optical Superlattices, Phys. Rev. Lett. **117**, 185301 (2016).
[77] S. Kolkowitz, S. L. Bromley, T. Bothwell, M. L. Wall, G. E. Marti, A. P. Koller, X. Zhang, A. M. Rey, and J. Ye, Spin-orbit-coupled fermions in an optical lattice clock, Nature (London) **542**, 66 (2017).
[78] M. L. Wall, A. P. Koller, S. Li, X. Zhang, N. R. Cooper, J. Ye, and A. M. Rey, Synthetic Spin-Orbit Coupling in an Optical Lattice Clock, Phys. Rev. Lett. **116**, 035301 (2016).
[79] C. A. Regal and D. S. Jin, Measurement of Positive and Negative Scattering Lengths in a Fermi Gas of Atoms, Phys. Rev. Lett. **90**, 230404 (2003).
[80] S. Gupta *et al.*, Radio-frequency spectroscopy of ultracold fermions, Science **300**, 1723 (2003).
[81] C. Chin *et al.*, Observation of the pairing gap in a strongly interacting Fermi gas, Science **305**, 1128 (2004).
[82] Y. Shin, C. H. Schunck, A. Schirotzek, and W. Ketterle, Tomographic rf Spectroscopy of a Trapped Fermi Gas at Unitarity, Phys. Rev. Lett. **99**, 090403 (2007).
[83] L. Jiang, L. O. Baksmaty, H. Hu, Y. Chen, and H. Pu, Single impurity in ultracold Fermi superfluids, Phys. Rev. A **83**, 061604(R) (2011).
[84] C. Reeg, C. Schrade, J. Klinovaja, and D. Loss, DIII topological superconductivity with emergent time-reversal symmetry, Phys. Rev. B **96**, 161407(R) (2017).